Supplemental Figure legends

Fig. S1: Absolute abundance of OMM^{12} bacteria during *S*. Tm infection. Related to Fig. 1 and 2.
Analysis of microbiota composition in fecal samples at different time points p.i.. Microbiota composition was determined by strain-specific qPCR assay and is shown as absolute abundances of the individual strains (16S rRNA gene copy numbers/µl genomic DNA). **(A)** *B. caecimuris* I48. **(B)** *M. intestinale* YL27. **(C)** *A. muciniphila* YL44. (**D**) *T. muris* YL45. (**E**) *L. reuteri* I49. (**F**) *E. faecalis* KB1. (**G**) *B. coccoides* YL58. (**H**) *C. innocuum* I46. (**I**) *F. plautii* YL31. (**J**) *E. clostridioformis* YL32. (**K**) *A. muris* KB18. (**L**) *B. animals* YL2.

Fig. S2: Microbiota composition in the course of *S*. Tm^{WT} and *S*. Tm^{avir} infection in OMM^{12} mice. (A) Analysis of microbiota composition in fecal samples at indicated time points. Microbiota composition was determined by strain-specific qPCR assay and is shown as relative abundances of the individual strains (% of cumulated 16S rRNA gene copy numbers). **(B)** PCoA based on the distance matrix of Bray-Curtis dissimilarity of relative OMM^{12} abundance profiles shows the effect of time after infection. Points are colored by time (days) after infection. **(C)** Relative abundance of *S*. Tm in cecal contents at different time points. **(D)** Absolute amount of 16S rRNA gene copies (determined by an universal primer / probe combination). Statistical analysis was performed using Kruskal-Wallis test with Dunn's multiple comparison test (* $p<0.05$, ** $p<0.01$, *** $p<0.001$). Each dot represents one mouse, black lines indicate median, grey lines indicate detection limit (DTL).

Fig. S3: *S.* Tm requires functional T3SS-1 and 2 to induce dysbiosis at day 4 p.i.. Experimental set-up: OMM^{12} mice were orally infected with 5 x 10^7 CFUs of either *S*. Tm^{avir} (Δ*invG*, *sseD*::*aphT*), *S*. Tm^{SPI-1} (Δ*invG*), *S*. Tm^{SPI-2} (*sseD*::*aphT*) or with *S*. Tm^{WT}. Data from infections with *S*. Tm^{avir} and *S*. Tm^{WT} originate from the previous experiment (Fig. 2). Mice were sacrificed at day 4 p.i. and samples were taken for analysis. There was also a fecal control sample taken before infection. **(A)** *Salmonella* loads in cecal content at day 4 p.i. (CFUs *S*. Tm / g content). **(B)** Lipolcalin-2 levels in cecal content at day 4 p.i. measured by ELISA (ng / mg cecal content). **(C)** Cecal pathology determined by evaluation of HE stained tissue sections. **(D)** Analysis of microbiota composition in feces (left) and cecal content (right) at day 4 p.i. with different *S.* Tm mutants. Microbiota composition is shown as relative abundance and expressed as % of cumulated 16S rRNA gene copy numbers (% of total 16S rRNA gene copies). The amount of absolute 16S rRNA gene copies (determined by an universal primer / probe combination) is illustrated as black dots (the right y axis). * Limit of detection. **(E)** Cluster analysis of fecal (upper section) and cecal (lower section) microbiota composition after infection with different *Salmonella* strains. The analysis is based on Pearson distance matrix visualized as PCoA plots. Grouping by infection with different *Salmonella* strains was significant (feces and cecal content: $p<0.001$, Adonis) with 86% (feces) and 85% (cecal content) of variation explained. PERMDISP analyses revealed statistically significant differences in microbiota composition after infection with *S*. Tm^{avir}, *S*. Tm^{WT} in feces and after

infection with *S*. Tm^{avir}, *S*. Tm^{SPI-1} and *S*. Tm^{WT} in cecal content (* p<0.05, ** p<0.01, *** p<0.001). **(F)** Systemic *Salmonella* loads in mesenteric lymphnodes, liver and spleen (CFUs per organ) at day 4 p.i.. Relative cecum weight at day 4 p.i. is expressed as % of body weight. Data are indicated as the median. Statistical analysis between groups was performed using Kruskal-Wallis test with Dunn's multiple comparison test (* p<0.05, ** p<0.01, *** p<0.001). # Animal that exhibited dysbiosis after infection with *S*. Tm^{SPI-2}. Dashed lines: DTL: limit of detection (mLN: 10 CFUs, liver: 60 CFUs, spleen: 20 CFUs).

Fig. S4: Organ loads and microbiota composition of OMM^{12} mice infected with *S.* Tm mutants in T3SS-1 and 2. Experimental setup: see Fig. S3. *S.* Tm loads in **(A)** mesenteric lymphnodes, **(B)** liver and **(C)** spleen at day 4 p.i. were determined by plating. Microbiota composition was determined by strain-specific qPCR assay and is shown as absolute abundances of the individual strains (16S rRNA gene copy numbers/μl genomic DNA). **(D)** *B. caecimuris* I48. **(E)** *M. intestinale* YL27. **(F)** *A. muciniphila* YL44. (**G**) *T. muris* YL45. (**H**) *L. reuteri* I49. (**I**) *E. faecalis* KB1. (**J**) *B. coccoides* YL58. (**K**) *C. innocuum* I46. (**L**) *F. plautii* YL31. (**M**) *E. clostridioformis* YL32. (**N**) *A. muris* KB18. (**O**) *B. animals* YL2.

Fig. S5: Organ loads of OMM^{12} mice infected with *S.* Tm mutants. Experimental setup: OMM^{12} mice were infected with *S*. Tm mutants deficient in nitrate respiration (*S*. Tm$^{Ni.;}$ Δ*narZ*; *narG*::*cat*; *napA*::*aphT*) and in nitrate and tetrathionate respiration (*S*. Tm$^{Ni. + Te.}$; Δ*narZ*; *narG*::*cat*; *napA*::*aphT*; *ttrS*::*tet*), salmochelin production (*S.* Tm *entA*::cat; *S.* Tm^{EntA}) and ethanolamine degradation (*eutC*::*aphT*; *S*. Tm^{EA}) and *S.* Tm^{WT} as control. *S.* Tm loads in **(A)** mesenteric lymphnodes, **(B)** liver and **(C)** spleen at day 4 p.i. were determined by plating.

Fig. S6: Course of infection of a *S.* Tm^{CyxA} mutant in OMM^{12} mice. OMM^{12} mice were orally infected with different *S.* Tm^{CyxA} (n=6) or S. Tm^{WT} (n=5). Mice were sacrificed at day 4 post infection **(A)** *S.* Tm loads in feces and cecal content at days 1, 3 and 4 post infection were determined by plating. **(B)** Histopathological analysis of cecal tissue at day 4 p.i.. Cecal tissue sections of the mice were stained with hematoxylin/eosin to determine the degree of submucosal edema, neutrophil infiltration and epithelial damage (1–3: no pathological changes; 4–6: moderate inflammation; above 7: severe inflammation). *S.* Tm loads in the mesenteric lymph nodes **(C)**, liver (**D**) and spleen (**E**). Analysis of microbiota composition in cecal content (**F**). Microbiota composition was determined by strain-specific qPCR assay and is shown as relative abundances of the individual strains (% of cumulated 16S rRNA gene copy numbers). **(G)** PCoA based on the distance matrix of Bray-Curtis dissimilarity of relative OMM^{12} abundance profiles shows the effect of the different *S*. Tm mutant strains. Points are colored by time (days) after infection. **(H)** Relative abundance of *S*. Tm and **(I)** absolute amount of 16S rRNA gene copies (determined by an universal primer / probe combination) in cecal contents 4 days p.i.. Statistical analysis was performed using Kruskal-Wallis test with Dunn's multiple comparison test (* p<0.05, ** p<0.01, *** p<0.001). Each dot represents one mouse, black lines indicate median, grey lines indicate detection limit (DTL).

Fig. S7: Absolute abundance of OMM^{12} strains in mice infected with *S.* Tm mutants. Related to Fig. 3 and Fig. S6. Analysis of microbiota composition in cecal content at day 4 p.i.. Microbiota composition was determined by strain-specific qPCR assay and is shown as absolute abundances of the individual strains (16S rRNA gene copy numbers/µl genomic DNA). **(A)** *B. caecimuris* I48. **(B)** *M. intestinale* YL27. **(C)** *A. muciniphila* YL44. (**D**) *T. muris* YL45. (**E**) *L. reuteri* I49. (**F**) *E. faecalis* KB1. (**G**) *B. coccoides* YL58. (**H**) *C. innocuum* I46. (**I**) *F. plautii* YL31. (**J**) *E. clostridioformis* YL32. (**K**) *A. muris* KB18. (**L**) *B. animals* YL2. Statistical analysis was performed using Kruskal-Wallis test with Dunn's multiple comparison test (* p<0.05, ** p<0.01, *** p<0.001). Each dot represents one mouse, black lines indicate median, grey lines indicate detection limit (DTL).

Fig. S8: Organ loads and microbiota composition of OMM^{12} mice treated with one dose of α-Ly6G antibody or isotype control and infected with *S.* Tm^{WT}. Experimental setup: see Fig. 4. *S.* Tm^{WT} loads in **(A)** mesenteric lymphnodes, **(B)** liver and **(C)** spleen at day 4 p.i. were determined by plating. Microbiota composition was determined by strain-specific qPCR assay and is shown as absolute abundances of the individual strains (16S rRNA gene copy numbers/µl genomic DNA). **(D)** *B. caecimuris* I48. **(E)** *M. intestinale* YL27. **(F)** *A. muciniphila* YL44. (**G**) *T. muris* YL45. (**H**) *L. reuteri* I49. (**I**) *E. faecalis* KB1. (**J**) *B. coccoides* YL58. (**K**) *C. innocuum* I46. (**L**) *F. plautii* YL31. (**M**) *E. clostridioformis* YL32. (**N**) *A. muris* KB18. (**O**) *B. animals* YL2. Light and dark gray arrows indicate samples analyzed at day 2 or 3 p.i., respectively. Statistical analysis was performed using Mann Whitney test (* p<0.05, ** p<0.01, *** p<0.001). Each dot represents one mouse, black lines indicate median, grey lines indicate detection limit (DTL).

Figure S1

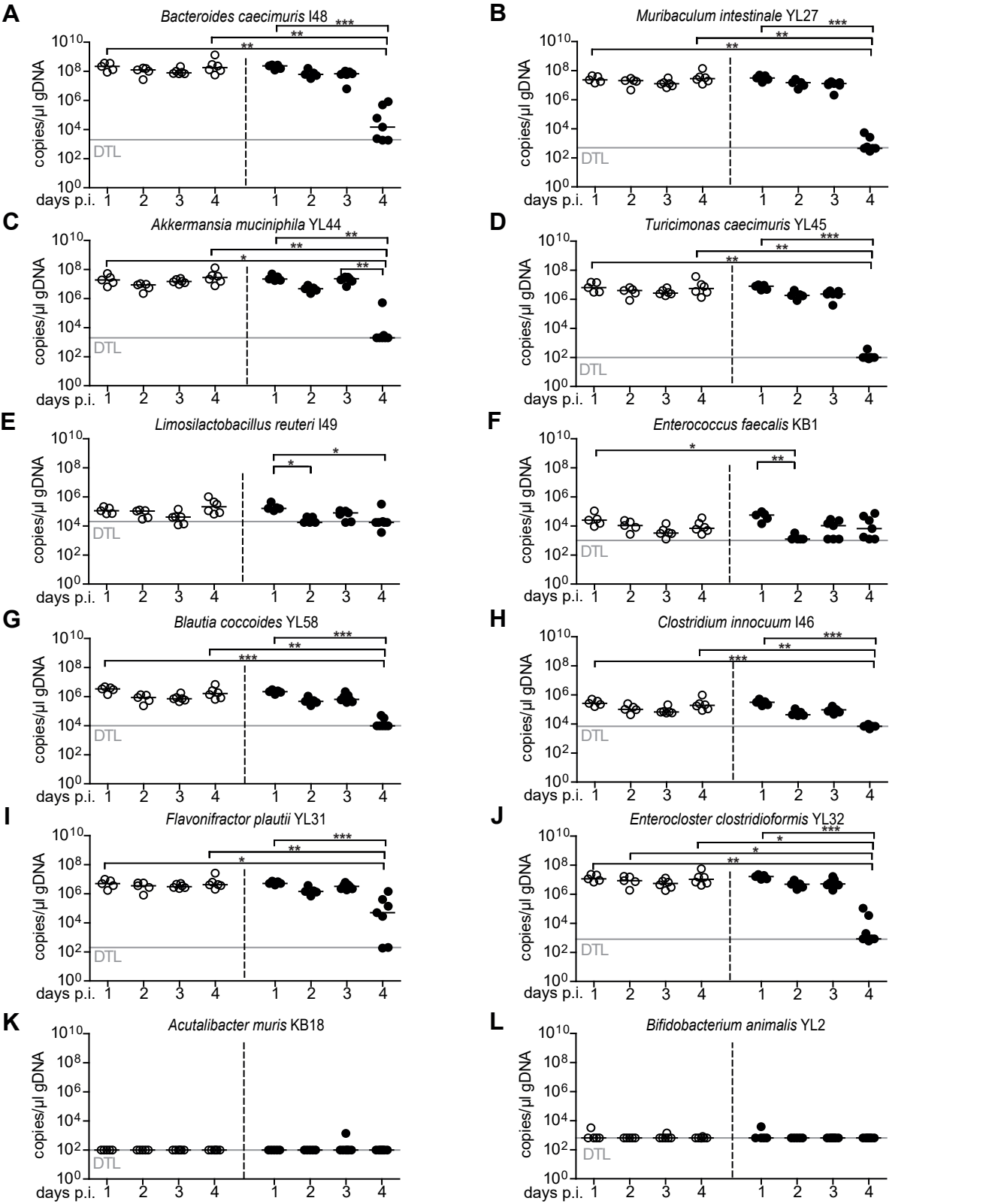
A
Bacteroides caecimuris I48
B
Muribaculum intestinale YL27
C
Akkermansia muciniphila YL44
D
Turicimonas caecimuris YL45
E
Limosilactobacillus reuteri I49
F
Enterococcus faecalis KB1
G
Blautia coccoides YL58
H
Clostridium innocuum I46
I
Flavonifractor plautii YL31
J
Enterocloster clostridioformis YL32
K
Acutalibacter muris KB18
L
Bifidobacterium animalis YL2
copies/µl gDNA
DTL
days p.i.

Figure S2

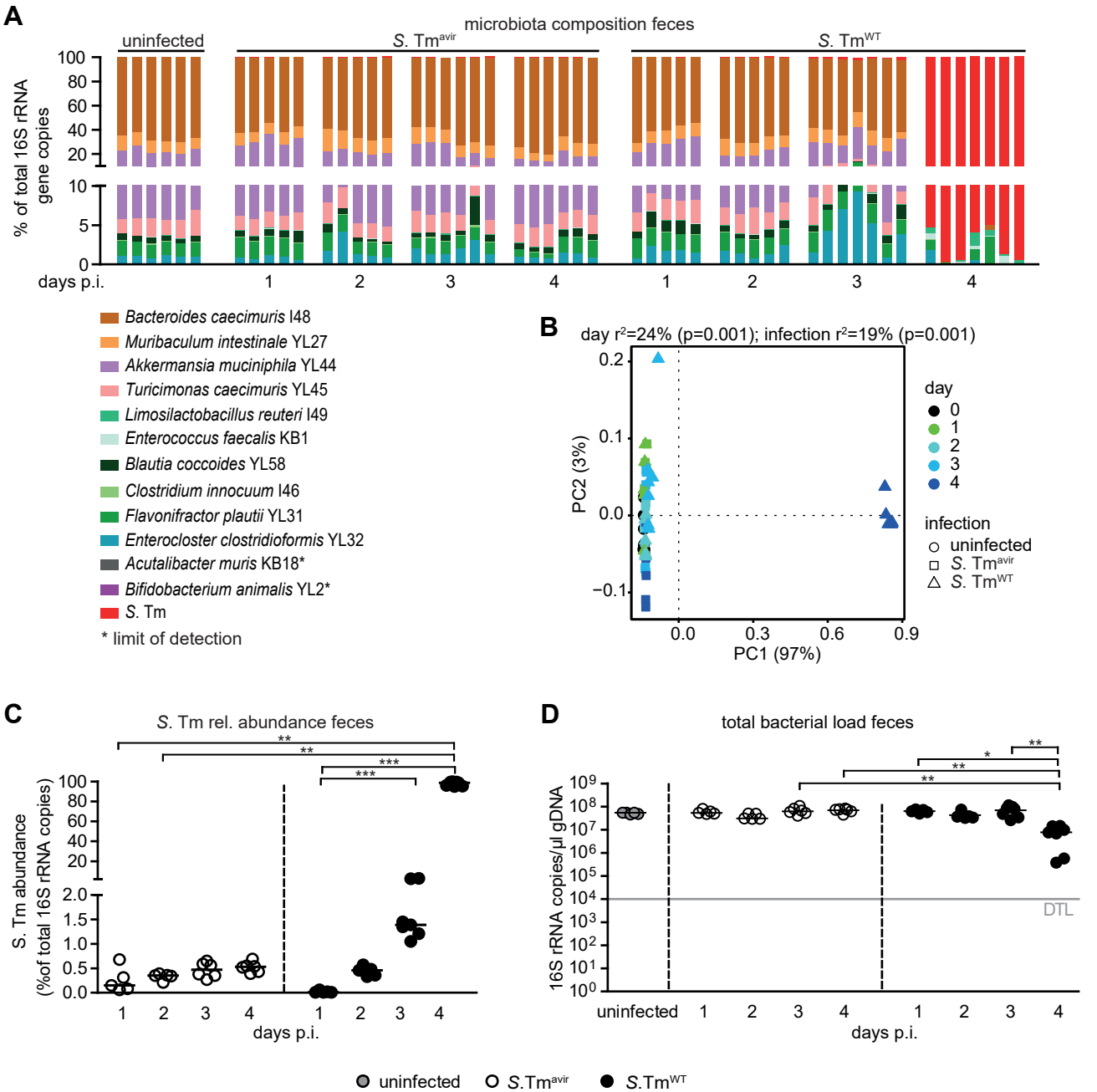
A
microbiota composition feces
uninfected
S. Tm^avir
S. Tm^WT
% of total 16S rRNA gene copies
days p.i.
Bacteroides caecimuris I48
Muribaculum intestinale YL27
Akkermansia muciniphila YL44
Turicimonas caecimuris YL45
Limosilactobacillus reuteri I49
Enterococcus faecalis KB1
Blautia coccoides YL58
Clostridium innocuum I46
Flavonifractor plautii YL31
Enterocloster clostridioformis YL32
Acutalibacter muris KB18*
Bifidobacterium animalis YL2*
S. Tm
* limit of detection
B
day r²=24% (p=0.001); infection r²=19% (p=0.001)
PC2 (3%)
PC1 (97%)
day
infection
uninfected
S. Tm^avir
S. Tm^WT
C
S. Tm rel. abundance feces
S. Tm abundance (%of total 16S rRNA copies)
days p.i.
D
total bacterial load feces
16S rRNA copies/µl gDNA
DTL
uninfected
days p.i.
uninfected
S.Tm^avir
S.Tm^WT

Figure S3

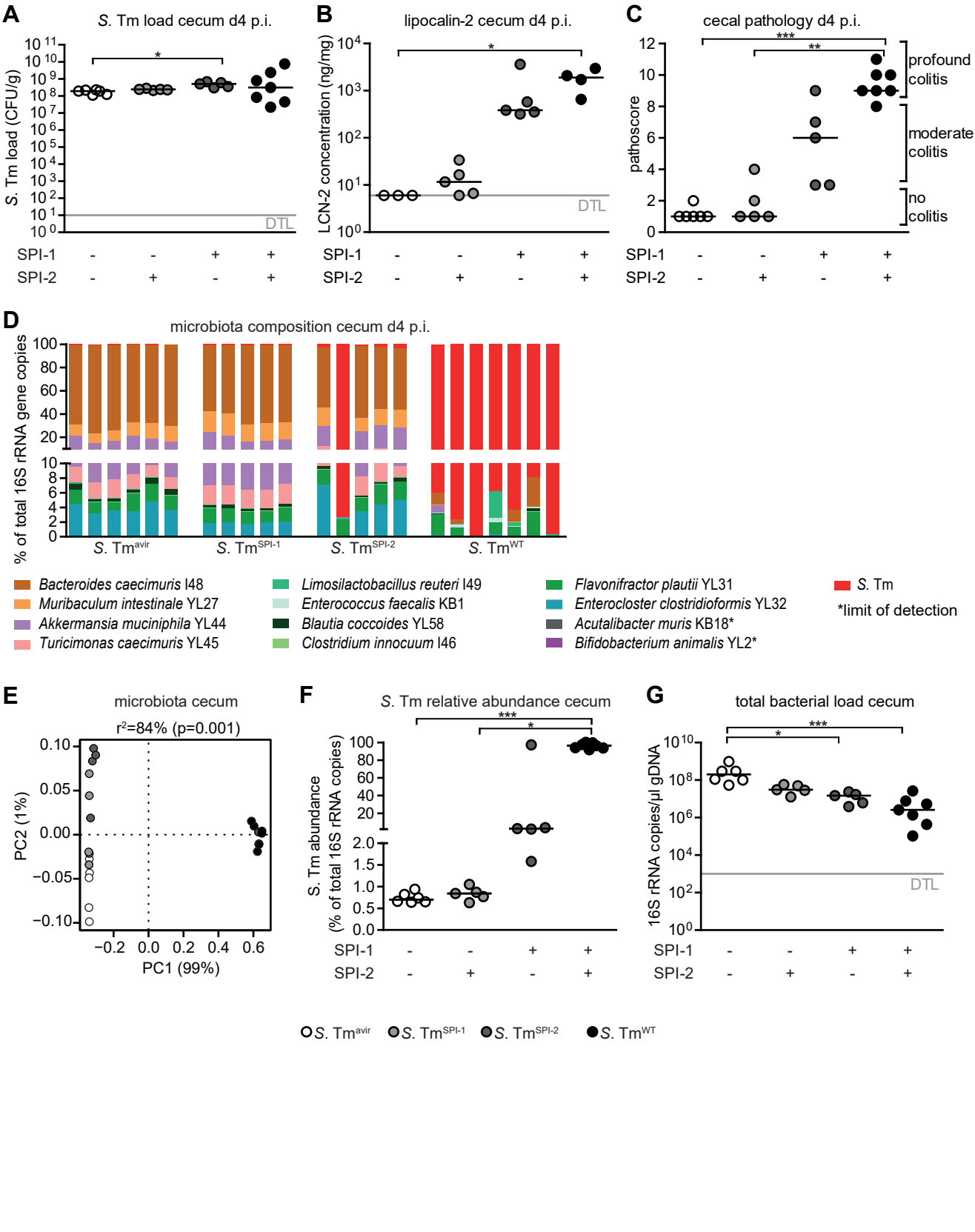
A
S. Tm load cecum d4 p.i.
S. Tm load (CFU/g)
DTL
SPI-1
SPI-2
B
lipocalin-2 cecum d4 p.i.
LCN-2 concentration (ng/mg)
DTL
C
cecal pathology d4 p.i.
pathoscore
profound colitis
moderate colitis
no colitis
D
microbiota composition cecum d4 p.i.
% of total 16S rRNA gene copies
S. Tm^avir
S. Tm^SPI-1
S. Tm^SPI-2
S. Tm^WT
Bacteroides caecimuris I48
Muribaculum intestinale YL27
Akkermansia muciniphila YL44
Turicimonas caecimuris YL45
Limosilactobacillus reuteri I49
Enterococcus faecalis KB1
Blautia coccoides YL58
Clostridium innocuum I46
Flavonifractor plautii YL31
Enterocloster clostridioformis YL32
Acutalibacter muris KB18*
Bifidobacterium animalis YL2*
S. Tm
*limit of detection
E
microbiota cecum
r²=84% (p=0.001)
PC2 (1%)
PC1 (99%)
F
S. Tm relative abundance cecum
S. Tm abundance (% of total 16S rRNA copies)
G
total bacterial load cecum
16S rRNA copies/µl gDNA
DTL
S. Tm^avir
S. Tm^SPI-1
S. Tm^SPI-2
S. Tm^WT

Figure S4

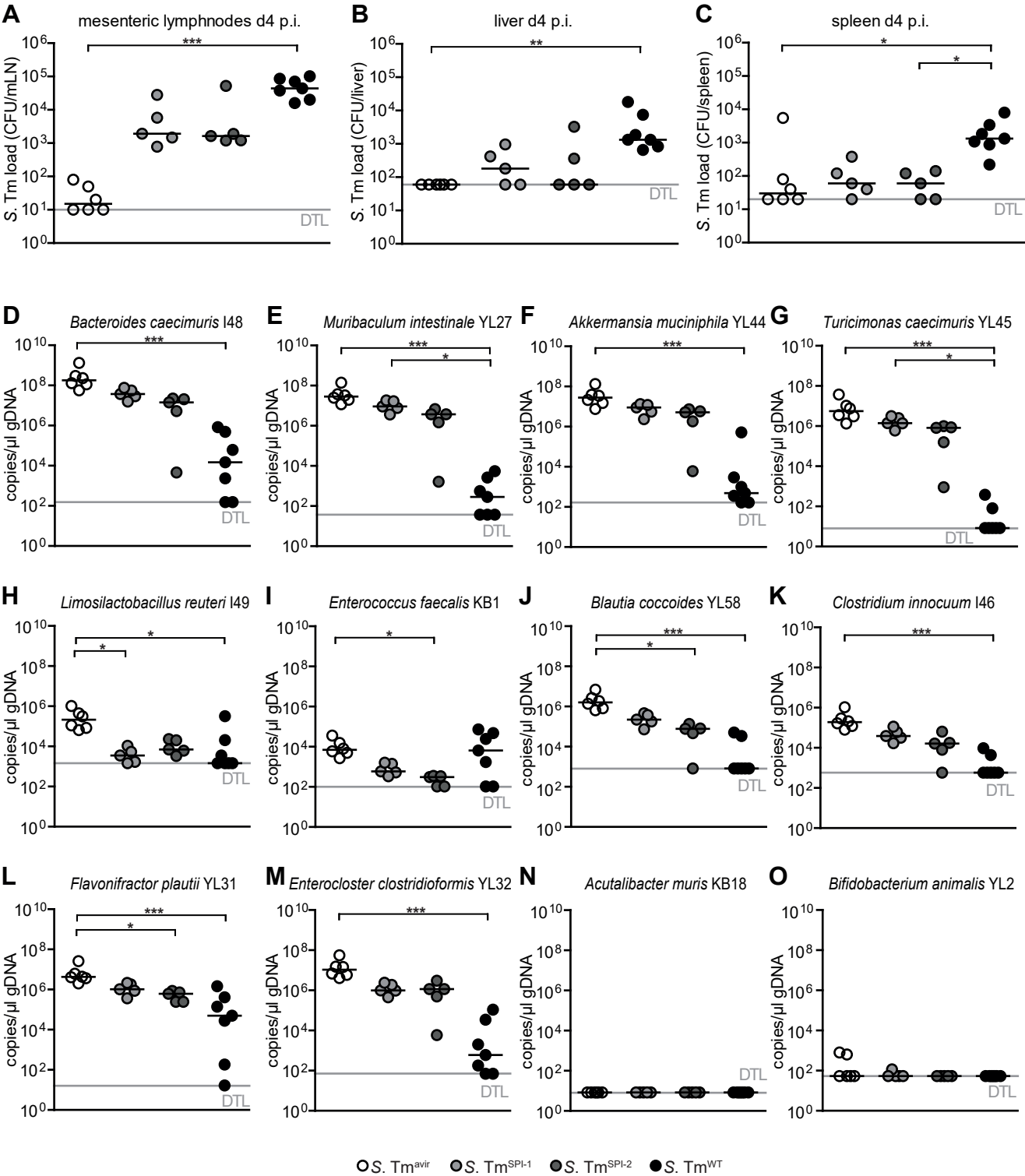
A
mesenteric lymphnodes d4 p.i.
S. Tm load (CFU/mLN)
B
liver d4 p.i.
S. Tm load (CFU/liver)
C
spleen d4 p.i.
S. Tm load (CFU/spleen)
DTL
D
Bacteroides caecimuris I48
E
Muribaculum intestinale YL27
F
Akkermansia muciniphila YL44
G
Turicimonas caecimuris YL45
H
Limosilactobacillus reuteri I49
I
Enterococcus faecalis KB1
J
Blautia coccoides YL58
K
Clostridium innocuum I46
L
Flavonifractor plautii YL31
M
Enterocloster clostridioformis YL32
N
Acutalibacter muris KB18
O
Bifidobacterium animalis YL2
copies/µl gDNA
S. Tmavir
S. TmSPI-1
S. TmSPI-2
S. TmWT

Figure S5

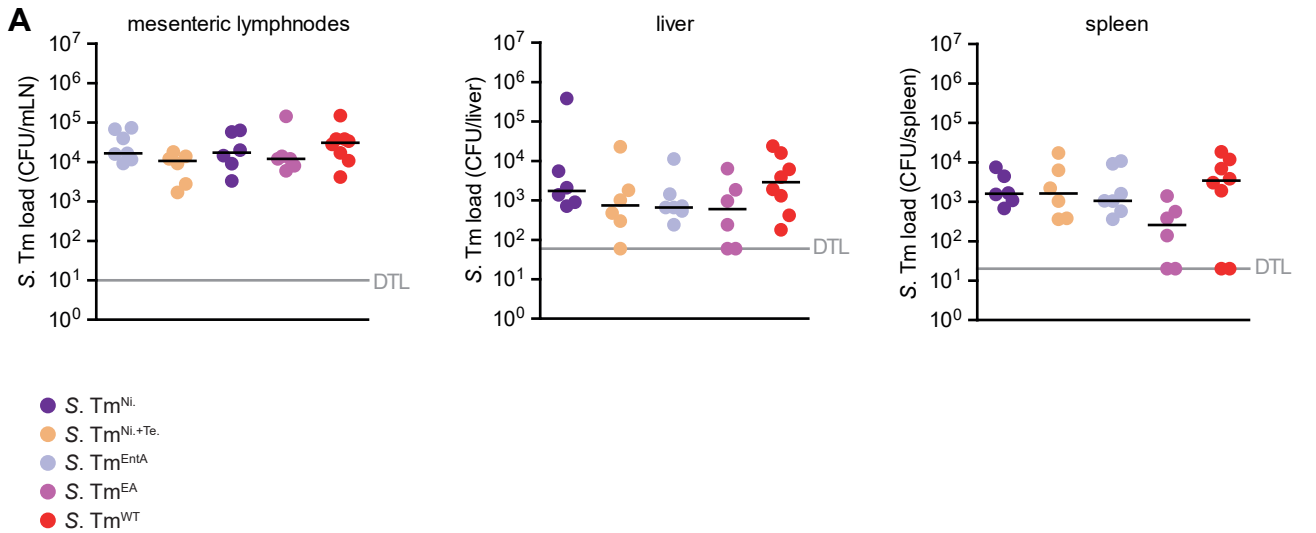
A
mesenteric lymphnodes
liver
spleen
S. Tm load (CFU/mLN)
S. Tm load (CFU/liver)
S. Tm load (CFU/spleen)
DTL
S. Tm^Ni.
S. Tm^Ni.+Te.
S. Tm^EntA
S. Tm^EA
S. Tm^WT

Figure S6

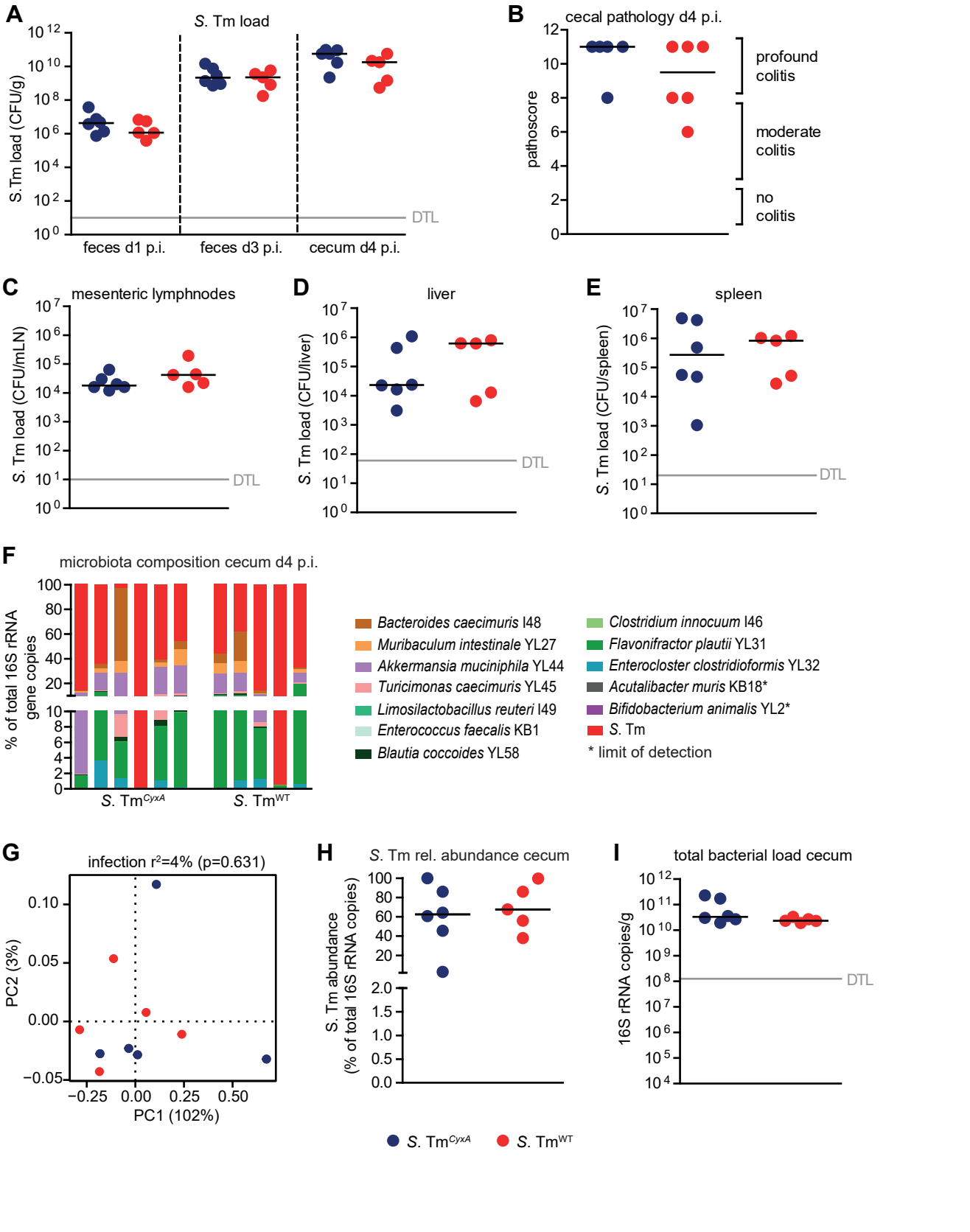
A
S. Tm load
S. Tm load (CFU/g)
DTL
feces d1 p.i.
feces d3 p.i.
cecum d4 p.i.
B
cecal pathology d4 p.i.
pathoscore
profound colitis
moderate colitis
no colitis
C
mesenteric lymphnodes
S. Tm load (CFU/mLN)
D
liver
S. Tm load (CFU/liver)
E
spleen
S. Tm load (CFU/spleen)
F
microbiota composition cecum d4 p.i.
% of total 16S rRNA gene copies
S. Tm^CyxA
S. Tm^WT
Bacteroides caecimuris I48
Muribaculum intestinale YL27
Akkermansia muciniphila YL44
Turicimonas caecimuris YL45
Limosilactobacillus reuteri I49
Enterococcus faecalis KB1
Blautia coccoides YL58
Clostridium innocuum I46
Flavonifractor plautii YL31
Enterocloster clostridioformis YL32
Acutalibacter muris KB18*
Bifidobacterium animalis YL2*
S. Tm
* limit of detection
G
infection r²=4% (p=0.631)
PC2 (3%)
PC1 (102%)
H
S. Tm rel. abundance cecum
S. Tm abundance (% of total 16S rRNA copies)
I
total bacterial load cecum
16S rRNA copies/g
S. Tm^CyxA
S. Tm^WT

Figure S7

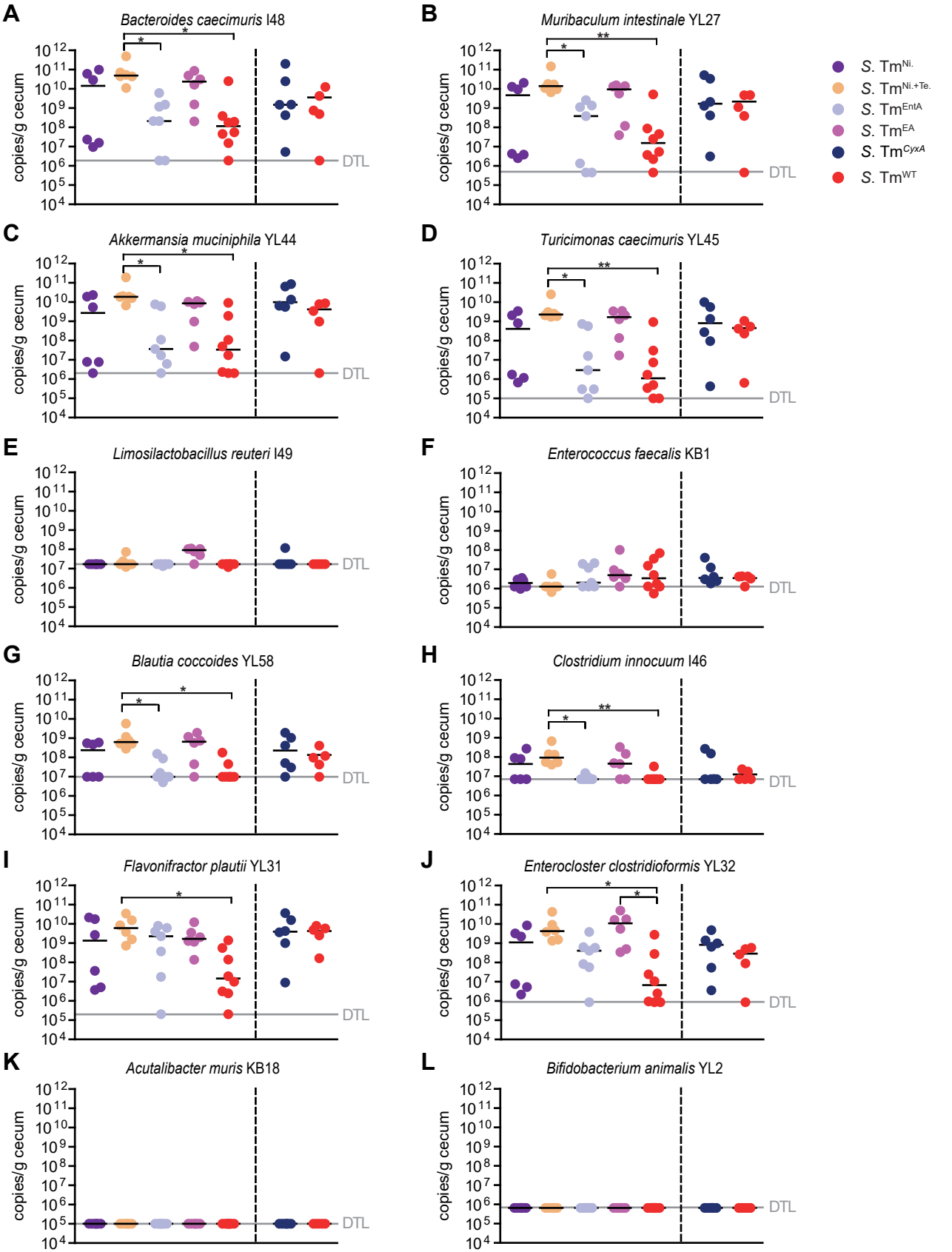
A
Bacteroides caecimuris I48
B
Muribaculum intestinale YL27
C
Akkermansia muciniphila YL44
D
Turicimonas caecimuris YL45
E
Limosilactobacillus reuteri I49
F
Enterococcus faecalis KB1
G
Blautia coccoides YL58
H
Clostridium innocuum I46
I
Flavonifractor plautii YL31
J
Enterocloster clostridioformis YL32
K
Acutalibacter muris KB18
L
Bifidobacterium animalis YL2
copies/g cecum
DTL
S. Tm^Ni.
S. Tm^Ni.+Te.
S. Tm^EntA
S. Tm^EA
S. Tm^CyxA
S. Tm^WT

Figure S8

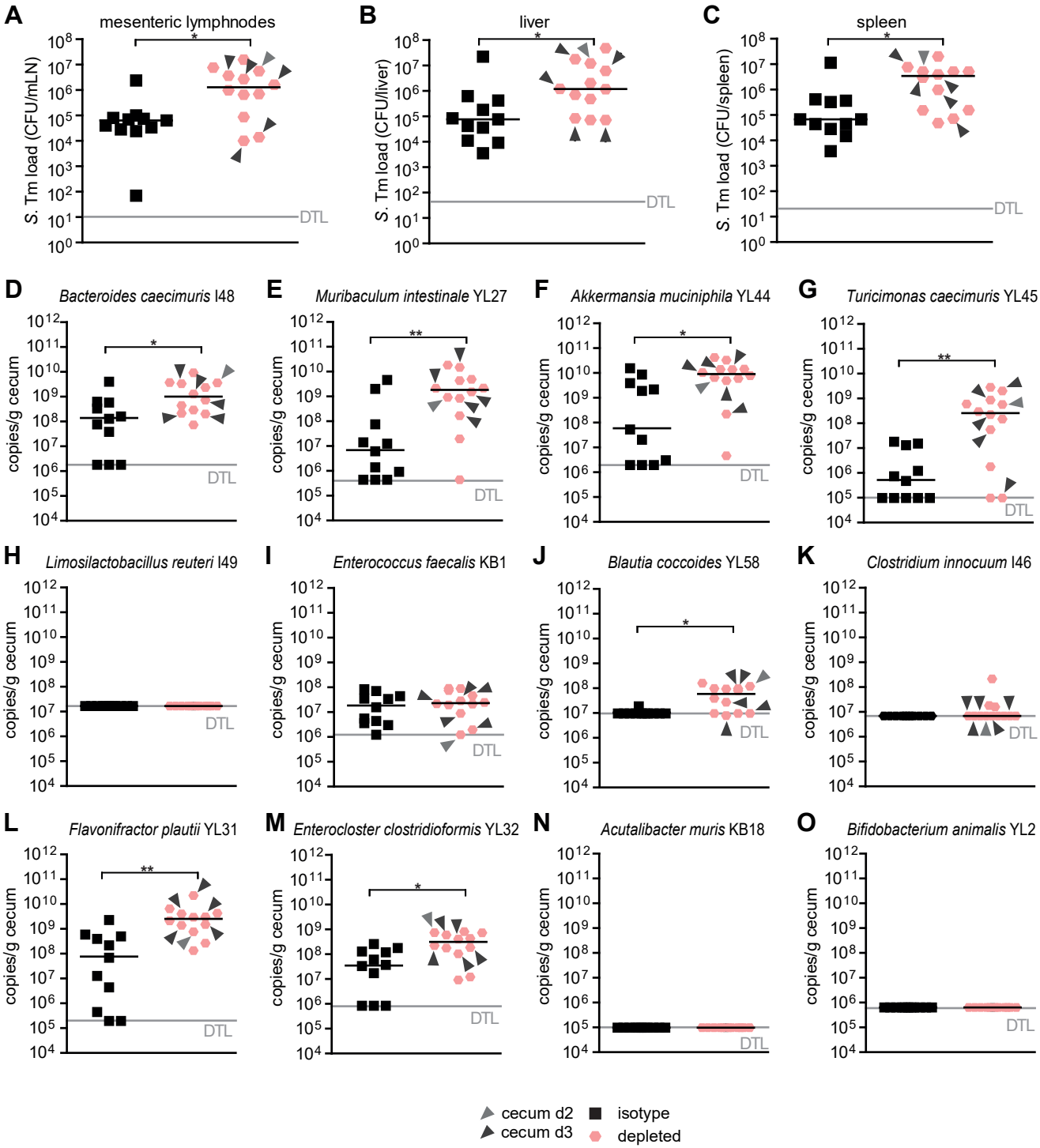
A
mesenteric lymphnodes
S. Tm load (CFU/mLN)
B
liver
S. Tm load (CFU/liver)
C
spleen
S. Tm load (CFU/spleen)
DTL
D
Bacteroides caecimuris I48
E
Muribaculum intestinale YL27
F
Akkermansia muciniphila YL44
G
Turicimonas caecimuris YL45
H
Limosilactobacillus reuteri I49
I
Enterococcus faecalis KB1
J
Blautia coccoides YL58
K
Clostridium innocuum I46
L
Flavonifractor plautii YL31
M
Enterocloster clostridioformis YL32
N
Acutalibacter muris KB18
O
Bifidobacterium animalis YL2
copies/g cecum
cecum d2
cecum d3
isotype
depleted